



University of Warwick institutional repository: <http://go.warwick.ac.uk/wrap>

This paper is made available online in accordance with publisher policies. Please scroll down to view the document itself. Please refer to the repository record for this item and our policy information available from the repository home page for further information.

To see the final version of this paper please visit the publisher's website. Access to the published version may require a subscription.

Author(s): Ian T. Pearson and J. Toby Mottram

Article Title: A finite element modelling methodology for the non-linear stiffness evaluation of adhesively bonded single lap-joints: Part 2.

Novel shell mesh to minimise analysis time

Year of publication: 2012

Link to published article:

<http://dx.doi.org/10.1016/j.compstruc.2011.10.006>,

Publisher statement: "NOTICE: this is the author's version of a work that was accepted for publication in Computers & Structures. Changes resulting from the publishing process, such as peer review, editing, corrections, structural formatting, and other quality control mechanisms may not be reflected in this document. Changes may have been made to this work since it was submitted for publication. A definitive version was subsequently published in Computers & Structures, VOL:90-91, , January 2012, DOI: 10.1016/j.compstruc.2011.10.006,"

I. T. Pearson and J. T. MOTTRAM, 'Finite element modelling methodology for the non-linear stiffness of adhesively bonded single lap-joints. Part 2. Novel shell mesh to minimise analysis time', *Computer and Structures*, pp. 8.

ISSN 0045-7949 doi:10.1016/j.compstruc.2011.10.006 (online)

A finite element modelling methodology for the non-linear stiffness evaluation of adhesively bonded single lap-joints. Part 2. Novel shell mesh to minimise analysis time

Ian T. Pearson¹ and J. Toby Mottram²

WMG¹ and School of Engineering²

Warwick University

Coventry CV4 7AL

ABSTRACT

A new modelling methodology is presented that enables the stiffness of adhesively bonded single lap-joints to be included in the finite element analysis of whole vehicle bodies. This work was driven by the need to significantly reduce computing resources for vehicle analysis. To achieve this goal the adhesive bond line and adherends are modelled by a relatively 'small' number of shell elements to replace the usual solid element mesh for a reliable analysis. Previous work in Part 1 has provided the necessary background information to develop and verify the new finite element analysis that reduces the solution runtime by a factor of 1000. Although a joint's non-linear stiffness is reliably simulated to failure load, it is recognised by the authors that the coarse shell mesh cannot provide accurate peak stresses or peak strains for the successful application of a numerical failure criterion. Given that the new modelling methodology is very quick to apply to existing shell models of vehicle bodies, it is recommended for use by the stress analyst who requires, say at the preliminary design stage, whole vehicle stiffness performance in a significantly reduced timeframe.

Key Words

¹ Corresponding author: E-mail I.T.Pearson@warwick.ac.uk

INTRODUCTION

The Finite Element (FE) method for stress analysis has been used extensively in the automotive industry over the past thirty years to predict the behaviour of bodies under driving conditions encountered during normally service life and accidental crash events [1 - 5]. Many of these computational investigations have been concerned with understanding the behaviour of spot-welded and weld/bonded structures [6 - 9] and have produced numerical outputs that correlated very well with data taken from measurement during laboratory testing.

Although FE methods have been successful in analysing the response of bonded single lap joints with configurations found in coupon strength testing, the manufacturers of vehicles have, for some time, desired a modelling methodology that can extend simulation work to usefully study the behaviour of complete bodies with bonded joints. To faithfully represent vehicle body stiffness requires a computational model that includes the adhesive layer, and this would seem to warrant a significant increase in the number of degrees of freedoms (by way of a very refined mesh of solid elements), resulting in solution times running into weeks. Because such lengthy runtimes are not commercially viable the authors have conducted a programme of research with the aim of developing a new modelling methodology that shall minimise the runtime for a FE analysis of a complete, adhesively bonded vehicle body.

The work presented in Part 1 [10] and Part 2 was executed in three distinct phases using the single lap-joint configuration subjected to tension loading (see Figure 1). All FE simulations were carried out using the ANSYS® finite element code. In stage one [10] a series of parametric laboratory tests was performed to quantify the influence of seven key parameters (these are identified in Figure 1) on the non-linear stiffness characteristics of bonded joints. In this work ‘joint stiffness’ is given by the tensile force divided by the displacement (appropriate to the gauge length in the laboratory series of tests) it produces in the direction of tensile loading. The measured results were used to validate the predictions from a FE model with a ‘coarse’ solid element mesh specification (having 0.24k degrees of freedom (d.o.f.) per unit width of joint). This acceptable solid element model was employed in stage two of the work [10] to further investigate non-linear stiffness behaviour by way of a parametric FE study that varied the key parameters in joint design. From this investigation additional insight into how the stiffness curves change (especially due to adherend flexure

and the formation and activation of plastic hinges at the overlap ends) was gained and the parameters essential in FE modelling for determining stiffness with confidence were identified. Using background information from the Part 1 investigations [10] the authors used stage three of the work to develop a novel model methodology for a very low number of d.o.f. per joint width. The simplified FE model shown in this paper is to give acceptable load-displacement results for the range of values to the key parameters found in vehicle construction.

BACKGROUND INFORMATION FROM PART 1 [10]

The initial part to the third stage of the research is to consider, and build upon, the background information that is reported in Part 1 [10], so that a decision can be made on whether or not each key parameter (see Figure 1) needs to be represented in the new modelling methodology.

The material non-linear relationship for the adhesive used in this investigation (2 part methacrylate MA 310) is defined by the true stress-true strain curve in Figure 2 and for the steel adherend (car body steel, BS steel) by the curve in Figure 3, and the modulus of elasticity for linear elasticity for the adhesive and for the adherend are listed in Table 1. The other key parameter values that are used to define the geometry of this ‘benchmark’ joint are listed in the first row to Table 2.

To establish whether or not a material’s non-linear response needs to be represented in the simplified shell model for single lap-joints the coarse solid element model of Part 1 was run (with a geometric non-linearity analysis) for the following three assumptions for the material true stress-true strain relationships:

1. Non-linear (for direct, and with shear properties calculated by the ANSYS® code) for the BS steel adherends and linear elasticity for the methacrylate adhesive (MA 310). This model is labelled in Figures 4 and 5 as Nst Lav, for Non-linear steel and Linear adhesive).
2. Linear elastic for steel and non-linear for the adhesive (label is Lst Nav)
3. Linear elastic for both steel and adhesive (Lst Lav).

Presented in Figure 4 are the three computational tension forces with displacement plots identified using the labels above, together with the full non-linear analysis curve (labelled Nst Nav) taken from Figure 15 in reference 10 and also, taken from Part 1, the mean laboratory test curve (from 10 specimen measurements) labelled 'Test'. As might be expected the Lst Lav and Lst Nav straight line curves are found to coincide and fail to predict the loss of joint stiffness that occurs when the adherends are subjected to load in excess of the steel's elastic limit. When compared with the steel non-linear material curves Nst Lav and Nst Nav the linear elastic predictions for joint stiffness are seen to be acceptable for the 'benchmark' joint parameters until the load P is > 3000 N, when localised yielding in the steel has developed. From the two pairs of curves in Figure 4 it is also evident that the stiffness of the 'benchmark' joint is little influenced by the adhesive's material constitutive relationship and consequently an analysis neglecting the material non-linearity of the adhesive materials would be acceptable to the requirements of the vehicle stress analyst. The analysis must include adherend material non-linearity if the applied load is sufficiently large to stress the adherend beyond its elastic limit.

Having determined the sensitivity of the 'benchmark' joint's response with geometric non-linearity the four material models were re-analysed in a small displacement analysis. The curves generated from this static study are given in Figure 5, and for the purpose of comparison the mean laboratory test curve (Test) from Figure 4 for the non-linear joint stiffness is also presented.

Comparing equivalent results from the large displacement analyses in Figure 4 with those from the small displacement analyses in Figure 5 it is found that the instantaneous joint displacement has a greater influence on the actual joint's non-linear stiffness than does a change in material stiffness due to yielding. The reason for this significant difference in stiffness characteristics is the development and activation of localised plastic hinges in the steel at the overlap ends [10].

In Part 1 the parametric FE study using a coarse solid element model was for the single lap-joint configuration. Presented in Figure 6 are two curves from a full non-linear analysis for P against axial displacement when the material of the tensile members is only BS steel. The upper straight line curve is for a tension strut with the same cross-sectional area as the

overlap-length in the ‘benchmark’ joint, whose thickness and width is defined in Table 2. The lower non-linear curve is for the ‘benchmark’ joint with steel adherends and employing an adhesive with the same properties as BS steel. The presence of the overlap ends lowers stiffness and as tension force increases from zero to that at point A the stiffness of the stepped unit is influenced by the inherent load path eccentricity. With ever increasing load, the ‘overlap’ region rotates and in doing so there is a reduction in the eccentricity and the ‘parasitic’ bending moment does not continue to grow proportional with load. While changing geometry has an influence on the non-linear stiffness the presence of the stress concentrations at the overlap ends allow the steel to there yield in a localised volume across the joint width. When the load is 1400 N (point B), the steel starts to yield and material non-linearity starts to influence the non-linear stiffness. When the load attains 2100 N (point C) there is a full development of plastic hinges at the two overlap ends and their activation causes joint rotation at their locations to cease. Increasing tension further, toward point D in Figure 6, it is found that joint stiffness continues to decrease as the volume of plasticity in the adherends continually grows. The material in the strut does not become plastic until P is $>8000\text{N}$ (320 N/mm).

Having reviewed the background information from Part 1 [10], and completed new FE analysis for the plots in Figures 4 to 6, we can confirm that the methodology for the simplified joint model:

1. must include the stepped nature of the joint’s geometry
2. must account for the geometric non-linear response
3. can assume the adhesive has a linear elastic stress-strain relationship.

It is further established from the plots in Figure 4 that providing the whole vehicle analysis does not reach loads to cause yielding in the adherend material this material can also be specified a linear elastic stress-strain relationship. Should the whole vehicle analysis require the calculation of body deformations sufficiently high to cause, in the bonded joint, regions of plasticity (see Figures 4 to 6) then the modelling methodology must include the material non-linearity of the adherend material.

THE SIMPLIFIED JOINT MODEL USING SHELL ELEMENTS

To simulate the non-linear stiffness response of joints with adhesive bonding with an acceptable computing time the number of d.o.f. per unit width of joint must be significantly reduced from 0.24k per mm for the ‘coarse’ solid element model used in Part 1 [10]. Clearly, the reduction will be limited to when the reliability of the computational results is compromised. The single lap-joint configuration of Figure 1 is therefore to be modelled using the smallest possible number of finite elements. Automobile bodies comprise curved thin panels and for whole vehicle simulations this structural form lends itself to being modelled with shell elements. This approach corresponds to the modelling methodology recommended by the Society of Automotive Engineers (SAE) [11].

To assist in developing the simplified model we can use the information presented in Part 1 [10] concerning a parametric investigation combining laboratory testing and FE analysis, where the key parameters (Figure 2 and Tables 1 and 2) that significantly influence joint non-linear stiffness were identified. From this work the authors established that the four key parameters of adherend thickness (t_1), adherend stress-strain relationship (M_{ah}), bond line thickness (t_a) and overlap length (l) must be included. It was further established that the other three key parameters (i.e. unsupported length (u), the adhesive stress-strain relationship (M_{av}) and width of joint (b)) do not need to be exactly modelled. It is noteworthy that joint stiffness per unit width was found to be unaffected by changes in width since this suggests the behaviour of actual body joints (perhaps a metre wide) can be predicted from knowing the stiffness characteristics of laboratory sized test coupons, say of width 25 mm or higher.

For all potential applications in whole vehicle body modelling, the joint representation is developed to accommodate adherend material non-linearity. However, the majority of joints are unlikely to be subjected to deformations large enough to cause localised adherend yielding and so analysis neglecting the material non-linearity of the metal adherends is likely to be acceptable. Nevertheless, it is recognised that under certain circumstances, an analysis utilising non-linear adherend material properties and geometric non-linearities may be desirable and so is included here.

The theoretical work of Volkersen [12] and Goland and Reissner [13] highlights the fact that a majority of the joint load is transferred between the two adherends and through the adhesive

layer towards the ends of the bonded overlap region. This important finding means it should be possible in the simplified FE model to replace the adhesive layer with a small number of elements located at the ends of the overlap. For the solid element models (with both the refined and much coarser mesh) used in the Part 1 FE work [10] this could be achieved by simply omitting solid elements from the adhesive volume known to transfer little of the tensile load. A similar modelling methodology may be used with a shell element model when all the elements lie in the plane of the joint. An alternative option requiring fewer shell elements was created by the first author [14] to give acceptable non-linear stiffness results. For this novel modelling methodology the adhesive is represented by shell elements rotated through 90° to the plane of the joint and as Figure 7 shows they are used to connect the adherends at their overlap ends, but not anywhere else along the bond line. In addition, Figure 7 shows an isomeric view of this simplified shell element model for the ‘benchmark’ joint geometry. The four shell elements for the adhesive material are those shaded grey colour.

A shell element type suitable for analysing ‘thin to moderately-thick shell structures’ [15] is employed. For general application a ‘general shell element’ is chosen so that it has an equivalent in other FE codes. Of the suitable elements offered, the ANSYS® first-order element SHELL181 is rectangular, having four corner nodes and six degrees of freedom per node (three translational and three rotational). The ANSYS® manual states this element is suitable for ‘*linear, large rotation, and/or large strain nonlinear applications. Change in shell thickness is accounted for in nonlinear analyses*’ [15]. Although the adherend and adhesive thicknesses remain constant for the problem under consideration the other analysis capabilities of SHELL181 that allow for stress stiffening, large deflections (for geometrical non-linearity) and large strain effects (for material non-linearity), have been shown in this paper, and in Part 1 [10], to have an influence on a joint’s non-linear stiffness response.

A modelling predicament when using shell elements is that their mid-planes are to be located at the adherends’ mid-plane. This imposed modelling feature guarantees the adhesive thickness is greater than it should be, by a depth equal to one adherend thickness (this is valid as long as the thickness of the two adherends is the same). This frequently encountered modelling challenge is commonly accounted for by modifying the modulus of elasticity of the adhesive. For this work it has been established from an evaluation of the FE parametric

study in Part 1 [10] that, once this modulus of elasticity exceeds a threshold value of 0.46 GPa (for a 5% stiffness reduction from the ‘rigid’ bond line situation), its actual value does not significantly affect the stiffness response given by the ‘benchmark’ joint and a full non-linear analysis. A reason for this finding is that the volume of adhesive that experiences yielding is relatively small and is localised to the two overlap ends. This means the axial deformation of the adhesive layer provides little displacement towards the joint’s flexibility and so its overall deformation can be assumed to be linear elastic. It is therefore concluded that there is no necessity in the simplified FE analysis to account for the actual stress-strain relationship of the adhesive material, as given in Figure 2 for product MA 310.

For the shell element model in Figure 7 the actual adhesive layer length (equal to the overlap length, l) is represented by half of its length lumped at each end of the overlap. This modelling option is depicted in Figure 8 with the shell elements possessing ‘volume’ for clarity. If a is the total length of the adhesive bond line shown in Figure 8, then 50% of the adhesive length ($a/2$) is modelled as existing beyond the joint overlap ends. The other 50% of the adhesive’s length is then effectively contained within the overlap length l . The sensitivity of joint stiffness to changes in a (as defined by the thickness of the shell elements representing the adhesive) was investigated [14] using FE analysis of the simplified model of Figure 7. Results are not presented herein because very little difference was found for variations of the shell element thickness from $0.4a$ to $1.4a$. To support the need for simplicity in the simplified FE modelling approach, it is recommended that the modelled bond line length (a) is specified to be equal to the joint overlap length (l), as illustrated in Figure 8.

Using the shell element mesh shown in Figure 7 a parametric study was carried out varying all the key parameters [14]. For the case of the ‘benchmark’ steel joint the FE P -axial displacement results are compared in Figure 9 with the mean load against displacement curve ‘Test’ from the laboratory test programme [10, 14]. It is to be understood that the load-displacement variations between individual specimens in a batch of 10 [14] is greater than the small difference seen between the mean test curve and the NLg NLM curve. The simulation curve from the full non-linear analysis is labelled NLg NLM and can be seen to give excellent correlation with the ‘Test’ curve, especially after the plastic hinges at the overlap ends have developed ($P > 3200$ N) and become active in allowing ‘free’ joint rotation. To the point where the influence of adherend yielding starts to govern, the ‘Test’ curve stiffness is correctly predicted when the FE analysis accounts for geometric non-linearity and assumes

the adherend is a linear elastic material (no yielding). This analysis gives curve labelled NLg Lm and is not a straight line. If a static analysis is performed the straight line curve obtained is given by Lg Lm. A much lower initial joint stiffness, than NLg Lm, is predicted and, as seen from the plots in Figure 9, no acceptable correlation with the ‘Test’ curve is achieved. Because this latter FEA cannot give relevant and reliable results it is concluded that a static analysis would not be recommended with the rotated shell modelling approach.

Figures 10 and 11 presented the same curves as in Figure 9 for changes of key parameters from the ‘benchmark’ values (Figures 2 and 3 and Tables 1 and 2). The results in Figure 10 are due to changing the unsupported length (u) from 50 to 65 mm and those presented in Figure 11 are due to changing the adhesive thickness from 0.3 to 1.6 mm. Comparing the four P -displacement curves in Figures 10 and 11, respectively, confirms the observations and finding from the comparison of the same results in Figure 9 for the ‘benchmark’ joint. The unreliability of the static analysis (Lg Lm) is magnified in Figures 10 and 11 as its too low stiffness, in the linear elastic region ($P < 3000$ N), is seen to increase. Because the geometric non-linear analysis with linear elastic materials (NLg Lm) follows the ‘Test’ curve to $P = 3000$ N in the three Figures 9 to 11 it is observed that joint rotation with increasing P increases the stiffness. This important finding is highlighted by the plots in Figure 11, which show a non-linear response, even for $P < 500$ N. The main finding from the results given in Figures 9 to 11 is that geometric non-linearity must be included in the FEA if there is to be confidence in the stiffness calculation.

An excellent correlation is achieved [14] for all parameters investigated except for bond line thickness (t_a). Now the predicted joint stiffness is found to be consistently low, and the simplified FE model could not give an acceptable correlation when t_a is > 0.6 mm [14]. To explain this finding we examined the adhesive stress distribution using the coarse solid element mesh [10] with t_a set at 0.3 and 3.0 mm. It is found that, for the smaller of these two thicknesses the maximum adhesive stress at the overlap ends is more than five times its value in the mid-overlap section, whilst for the much deeper adhesive layer the maximum stress is less than four times higher. It can therefore be seen that as t_a increases less of the load is transferred in the region close to the overlap ends and more is transferred by the central region. To cope with this new modelling challenge the rotated shell representation of Figure 7 was modified to include a third shell element plane at the centre of the overlap

length. This modelling solution is shown in Figures 12 and 13 that are equivalent to Figures 7 and 8 when the extra plane of shell elements is not necessary. Evaluation of the results from the solid element simulations of Part 1 [10] confirmed that about 10% of the load is transferred in the central region and so the adhesive lengths in the simplified representation with three shell planes is specified to reflect this distribution. Good correlation was now achieved [14] without the restriction on the bond line thickness as is the case if the simplified model corresponds to that shown in Figure 7. The final mesh for the novel modelling approach is shown in Figure 12 and to represent the ‘benchmark’ joint geometry (first row in Table 2) it has 66 SHELL181 shell elements (or 0.023k d.o.f. per unit joint width). For no serious loss in calculating the non-linear stiffness response the reduced number of d.o.f. can be very favourably compared with the 0.24k d.o.f per unit width required in the ‘coarse’ solid element used in Part 1 of the work [10].

For application of the new modelling methodology in whole vehicle body analysis it is recommended that:

1. the FE analysis involves geometric non-linearity.
2. a linear elastic material model is used for the adhesive and for the metallic adherends if the affect on stiffness of adherend yielding is not a design requirement.
3. a full non-linear FE analysis is used if there is to be gross yielding adjacent to the overlap ends.
4. the adhesive layer can be replaced by shell element planes, rotated through 90° and placed on edge, with two planes at the overlap ends. For this simplification to be acceptable the total ‘thickness’ of these shell planes is to be at least the overlap length.
5. for joints with a thick bond line (say ≥ 0.6 mm) a third plane of shell elements is to be located at the mid-length of the overlap section.

Implementing these modelling recommendations into existing FE models for analysing body deformations will significantly reduce the number of d.o.f. needed, and thereby significantly reduce the analyst’s requirement for computing resources. By employing the simple mesh for a bonded lap-joint shown in either Figure 7 or 12 the required deformation of vehicle bodies can be commercially obtained. Additionally, any bonded joint region in a vehicle model that is identified in the design process as not having the desired stiffness can have this stiffness

modified by changing one or more of the four key parameters (t_1 , M_{ah} , l or t_a), and the results of Part 1 [10] will aid the decision making process.

To further add confidence to the application of the new modelling methodology it is shown in the PhD thesis by the first author [14] that there is no difference in the FE results if the shell element is quadratic (i.e. second-order). The presences of eight nodes per element increases the active d.o.f. from 335 (Figure 12) to 963. Additionally, the mesh in Figure 12 has only a single shell element in the plane for the adhesive thickness, and this eliminates from the analysis an out-of-plane curvature. Prediction of stiffness in [14] using a mesh with four elements through the bond line thickness (for both 4- and 8- noded shell elements) also shows no significant stiffness change from the simplified model presented in this paper.

OUT-OF-PLANE AND OTHER LOADING CASES

Because single lap-joints are principally designed to be subjected to in-plane loading, a tensile force has been considered in this work. Over the service life of a vehicle its body might be subjected to other forms of action, and so the out-of-plane stiffness response is not to be ignored. There is not space in this paper to report FE results for out-of-plane loading. Needless-to-say it can be shown [14] that the new simple model methodology gives a representation that can be used to calculate this joint stiffness with confidence.

Other loading cases can be identified that the simplified joint model would need to simulate. It should be understood that the new model is for a joint where a majority of the load is either transferred by shear loading across the adhesive layer or by a force acting parallel to the adhesive shell planes (i.e. for out-of-plane loading case). Because other loading cases, such as due to torsion and in-plane shearing, do not deform the adhesive in either of these two distinct ways the FE analysis with the rotated shells will need to be evaluated for these cases to.

APPLICATION OF NEW MODELLING METHODOLOGY

The new modelling methodology that uses rotated shells for the adhesive layer (see Figures 7 and 12) can be incorporated in whole vehicle models by applying the following four modelling steps:

1. The adhesive volume is represented by planes of shell elements placed at both overlap ends, and if adhesive layer is relatively thick by a third plane at middle of the overlap length. These element planes are rotated to be perpendicular to the joint itself, and are connected to the adherend shell elements as shown in Figure 12.
2. The total thickness of these shell element planes is chosen to give the same volume of adhesive (the total adhesive length being maintained) (see Figure 13). Should a third plane be located at the middle of the overlap the adhesive length should be distributed with 45% at both overlap ends and 10% at the middle. Should there be no middle plane the two end planes are assigned with 50% of the bond length. This latter modelling option is only valid if the adhesive thickness is less than 0.6 mm.
3. The mesh density for the lap-joint is specified as it would be in any FE model [16, 17] to include sufficient d.o.f. to simulate bending, and other deformations, and to ensure a smooth and continuous change in the strains and stresses between adjacent elements.
4. The adhesive is modelled using the linear elastic constitutive model requiring only knowledge of the elastic constants of modulus of elasticity and Poisson's ratio. Because joint stiffness is not sensitive to changes in the adhesive's modulus of elasticity, (providing its value exceeds 0.46 GPa for an estimated difference of 5% [10]) a value of 1.5 GPa is recommended, the analysis can use manufacturers' nominal listed values that are typically between 2 and 3 GPa.

CONCLUSIONS

To develop a finite element modelling methodology using the fewest shell elements to simulate the stiffness response of bonded single lap-joints in full vehicle body analysis it was necessary [10] to utilise information from the evaluation of results from a series of laboratory tests and finite element analyses with solid element meshes. Assessment of the finite element results from the parametric studies in [10] showed that it is difficult to establish a rank order for the seven key parameters that influence joint stiffness to failure. For the lap-joint configuration studied it is established that initial stiffness increases on: increasing adherend thickness; increasing the adherend modulus of elasticity; decreasing the bond line thickness and decreasing the overlap length. Stiffness is shown not to be significantly affected by varying the three key parameters of the adhesive's modulus of elasticity (providing a threshold had been exceeded) and the joint's unsupported length and width. It is also found

that any FE model of the bonded joint must include geometric non-linearity and only requires material non-linearity of the adherend material to be included if the loading is higher enough to activate plastic hinges at the overlap ends.

A very good correlation between finite element results (using a ‘coarse’ solid element model and ANSYS® software) and stiffnesses measured by a series of laboratory tests provided the information for this paper to validate the performance of a new shell element model having the fewest number of elements. The novelty of this approach is to model the adhesive by a very small number of shell elements rotated by 90° from plane of joint’s layers to create two or three shell planes. In this paper this simplified model is shown to predict the non-linear stiffness response with a substantive level of correlation. Sufficient reliability in stiffness predictions has been achieved by creating a shell mesh that possesses 230 degrees of freedom per millimetre width of joint. This represents a reduction of 94% from a coarse solid element model that probably does not have sufficient mesh refinement for acceptable stress predictions. The major benefit of minimising the number of active degree of freedom is to have run times 1/1000th of what is required to analysis the solid element model in Part 1 to this work.

The new model methodology can readily be included into existing shell element meshes for whole vehicle models that are used to analyse how bodies deform and failure, but, which could not previously involve bonded single lap-joints. It still remains the stress analyst’s responsibility to ensure that the modelling methodology is appropriate for the specifications of vehicle body analysis. One challenge to overcome with the new modelling approach presented in this paper is that its stress output is currently unacceptable for failure analysis. Work considering stress analysis of adhesively bonded joints, using standard FE techniques has recently been published by Castagnetti and Dragoni [18] and may be of help in this area. Further work is required to define the limitations for using the simply modelling methodology by way of restrictions on the range of valid joint’s key parameters and on how the analysis can cope with other loading cases, such as torsion.

Table 1. Linear elastic properties of benchmark adhesive and adherend used for bonded joints.

| | MA 310 | BS steel |
|-------------------------------------|--------|----------|
| Young's Elasticity (GPa) | 2.1 | 196 |
| Strain at limit of elasticity | 0.01 | 0.0009 |
| Stress at limit of elasticity (MPa) | 25.7 | 176 |

Table 2. Parameters for finite element parametric studies.

| | Width b (mm) | Adherend thickness t_1 (mm) | Overlap length l (mm) | Unsupported length u (mm) | Adhesive material M_{av} (GPa) | Adhesive thickness t_a (mm) | Adherend material M_{ah} (GPa) |
|-------------------|-------------------|-------------------------------------|-------------------------------|-----------------------------------|--|-------------------------------------|--|
| Benchmark | 25 | 0.8 | 20 | 50 | 2.1 | 0.3 | 196 |
| Variant values | 40, 60, 80 | 1.2, 1.6, 2.0 | 30, 55, 100 | 65, 100, 150 | 5.8, 2.9, 0.58 | 1.6, 2, 3 | 471, 68.7, 58.5 |

REFERENCES

- [1] W. C. Carpenter, *Two Finite Elements For Modelling The Adhesive In Bonded Configurations*. J Adhesion. 30 (1989) 25-46.
- [2] D. A. Wagner , *FEA (Finite Element Analysis) Modeling for Body-In-White Adhesives*. SAE 960784 (1996).
- [3] Y. M. Moon, T. H. Jee, Y. P. Park, Development of an Automotive Joint Model Using an Analytically Based Formulation, J Sound Vib 220(4) (1999) 625-640.
- [4] S. Steidler, Structural modelling of adhesive joints in automotive bodies, PhD, Oxford Brookes (2000).
- [5] T. Wang, O. S. Hopperstad, P. K. Larson, O. G. Lademo, *Evaluation of Finite Element Modelling Approach for Welded Aluminium Structures*. WIT Transactions for Engineering Science, 49. ISSN 1743-3533. WIT Press 2005.
- [6] I. J. M^cGregor, D. Nardini, Y. Gao, D Meadows, *A Joint Design Approach for Aluminium Structures*. Automot Eng (August 1993) 49-53.
- [7] Gilchrist and R. A. Smith, *Development of Cohesive Fatigue Cracks in T-Peel Joints*. Int J Adh Adh, 13(1) (1993).
- [8] T. Jones, N. Williams, *The Fatigue Properties of Spot Welded, Adhesive Bonded and Weld-Bonded Joints in High-Strength Steels*. SAE Technical Paper 860583, Michigan, (1986).
- [9] H. Kitagower, Y. Yoshida, *A Study of Bending and Torsion Rigidities of Weld Bonded Structures*. JSAE Rev 13(4) (October 1992) 72-76.
- [10] I. T. Pearson, J T. Mottram, *A finite element modelling methodology for the non-linear stiffness of adhesively bonded single lap-joints. Part I. Evaluation of key parameters*. Computers and Structures (2011)
- [11] D. A. Wagner, *FEA (Finite Element Analysis) Modeling for Body-In-White Adhesives*. SAE 960784 (1996).
- [12] O. Volkersen, *Die Nietkraftverteilung in Zugbeanspruchten Nietverbindungen Mit Konstanten Laschenquerschnitten (Rivet Strength Distribution in Tensile-Stressed Rivet Joints With Constant Cross Section)*. Luftfahrtforschung, 15 (German language) (1938).
- [13] M. Goland, E. Reissner, *The Stresses in Cemented Joints*. J Appl Mech, Trans ASME, 66 (1944) A17-A27.
- [14] I. T. Pearson, *A Method For The Inclusion Of Adhesively Bonded Joints In The Finite Element Analysis Of Automobile Structures*. PhD Thesis, University of Warwick. (2006)
- [15] ANSYS Version 10.0. *Element Reference*, Ch 4 Element Library. Swanson Analysis Systems Inc. PO Box 65, Johnson Road, Houston, PA 15342-0065. (2005).
- [16] G. Richardson, A. D. Crocombe, P.A. Smith, *A Comparison of two- and three-Dimensional Finite Element Analyses of Adhesive Joints*. Int J Adhes Adhes, 13(3) (1993) 193-2000
- [17] *A Finite Element Primer*, National Agency for Finite Element Methods and Standards, East Kilbride, ISBN 0 903640 17 1 (1986).

- [18] D. Castagnetti, E. Dragoni, *Standard finite element techniques for efficient stress analysis of adhesive joints* - Int J Adhes Adhes 29 (2009) p125-135.

Figure captions

- Figure 1. Joint parameters effecting stiffness response.
- Figure 2. Non-linear MA 310 material curves for FEA.
- Figure 3. True stress/strain relationships for BS Steel adherend materials in the FEA.
- Figure 4. Geometric non-linear analysis of ‘benchmark’ lap-joint with four material models.
- Figure 5. Static analysis of ‘benchmark’ lap-joint with four material models.
- Figure 6. Axial displacement of solid steel members showing influence of stepped geometry in single lap-joints.
- Figure 7. Simplified FE model with rotated shell elements for the adhesive layer.
- Figure 8. Incorporation of bondline length (l) in simplified FE model.
- Figure 9. Stiffness of “benchmark steel joint” using the shell element modelling methodology.
- Figure 10. Stiffness of steel joint with increased unsupported length (65 mm) using the shell element modelling methodology.
- Figure 11. Stiffness of steel joint with increased bondline thickness (1.6 mm) using the shell element modelling methodology.
- Figure 12. Simplified model with a shell element plane at the middle of overlap section when $t_a \geq 0.6\text{mm}$.
- Figure 13. Bond line length distribution when there is a third shell plane at the middle of the overlap section.

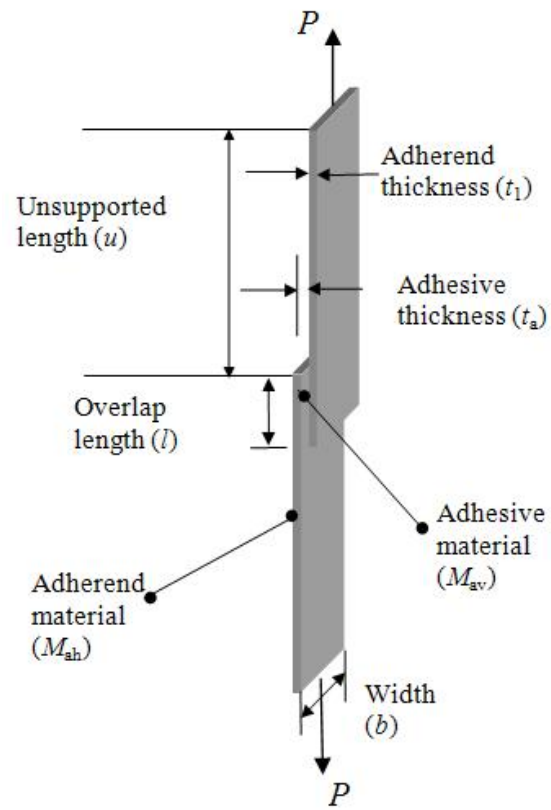


Figure 1

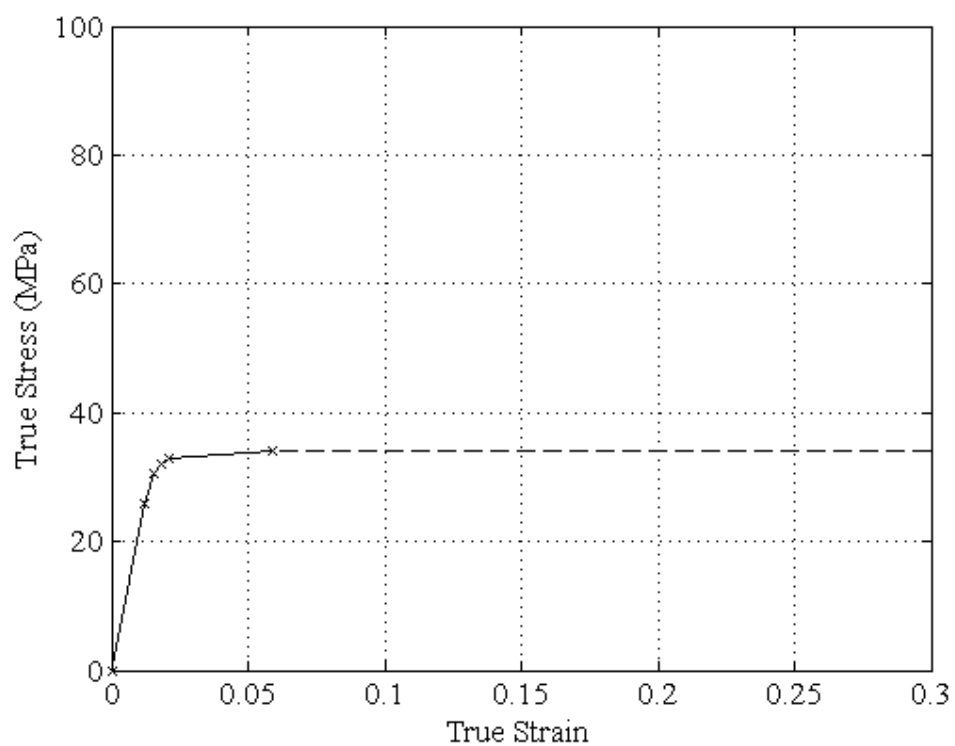


Figure 2

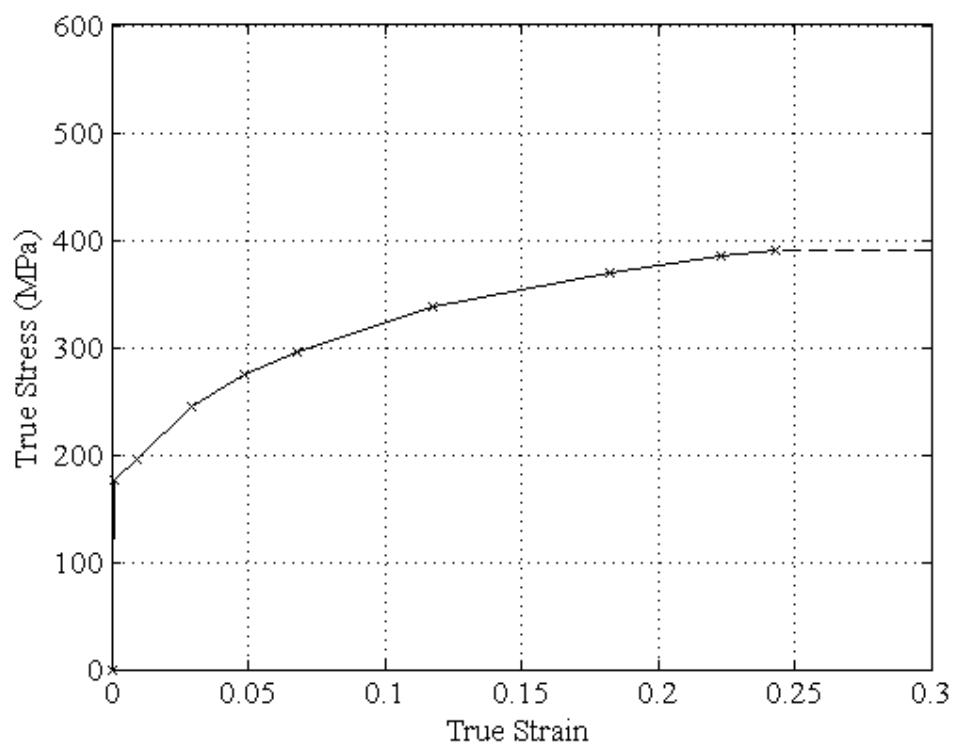


Figure 3

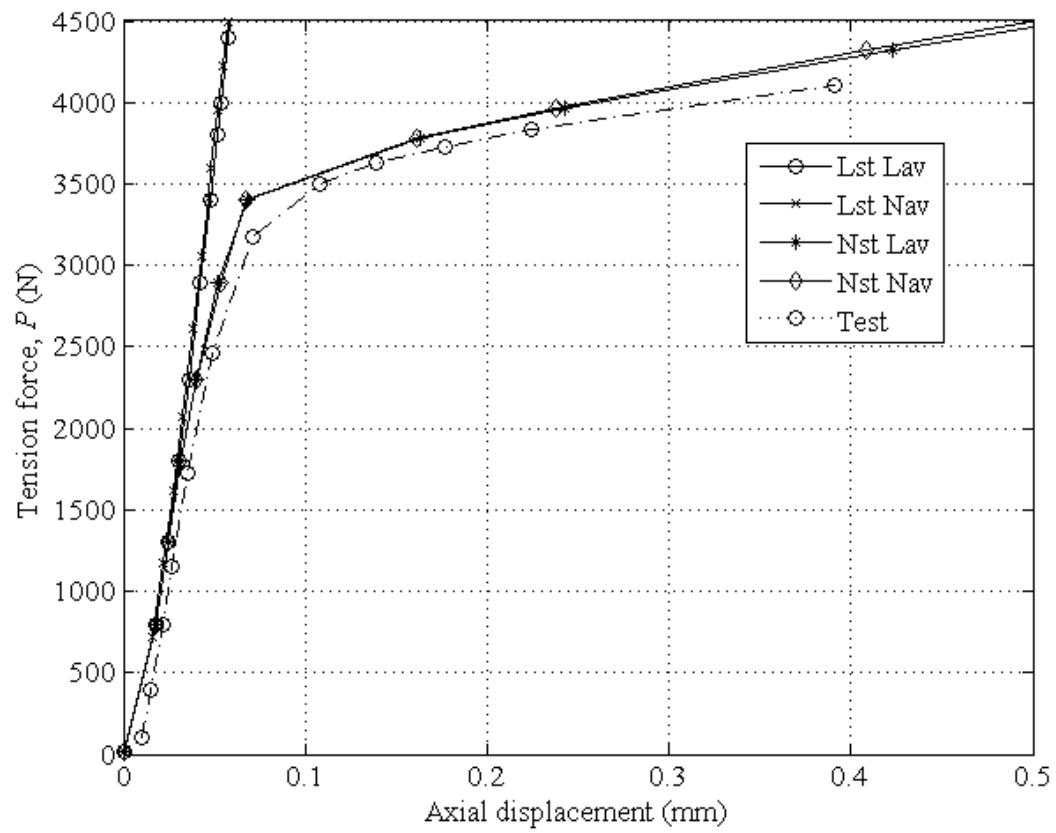


Figure 4

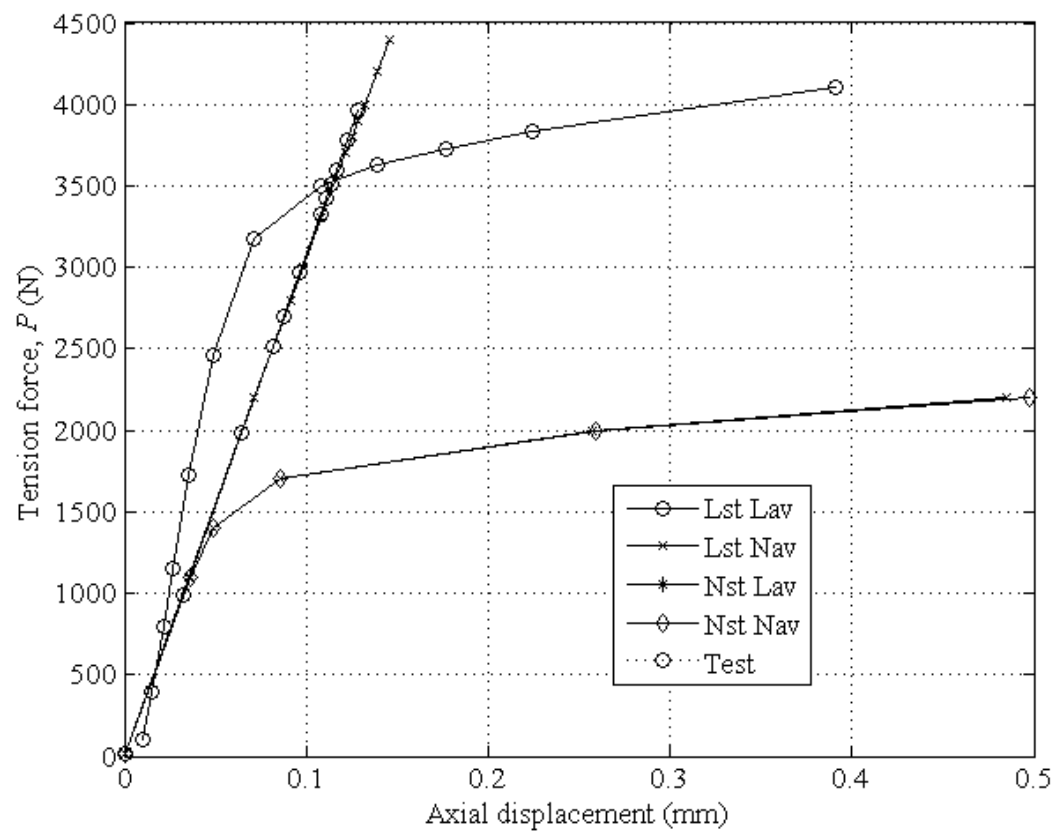


Figure 5

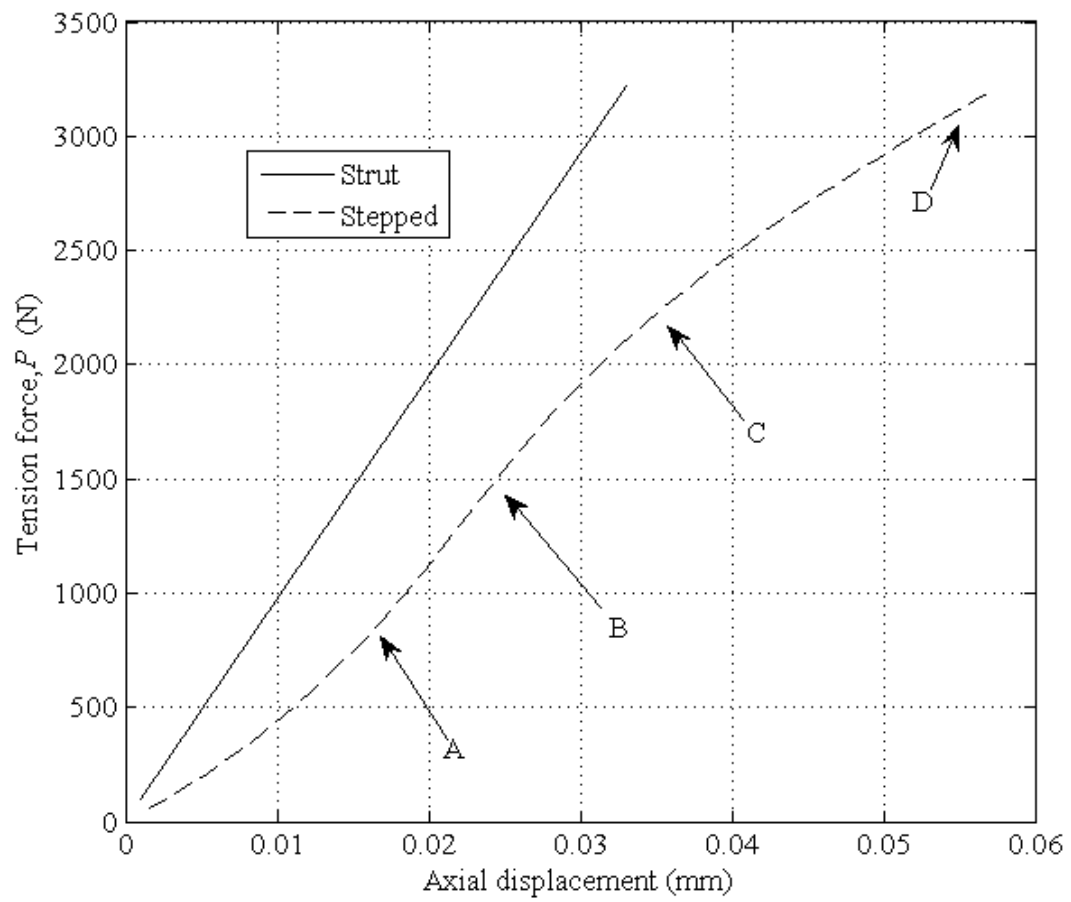


Figure 6

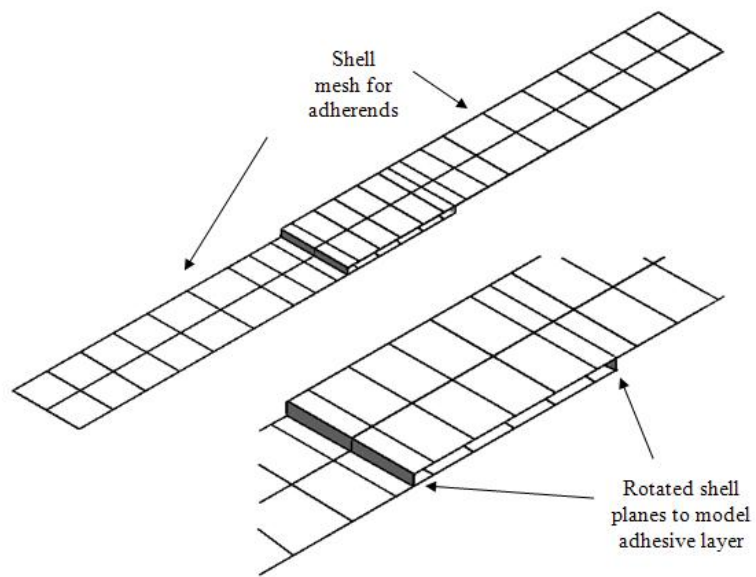


Figure 7

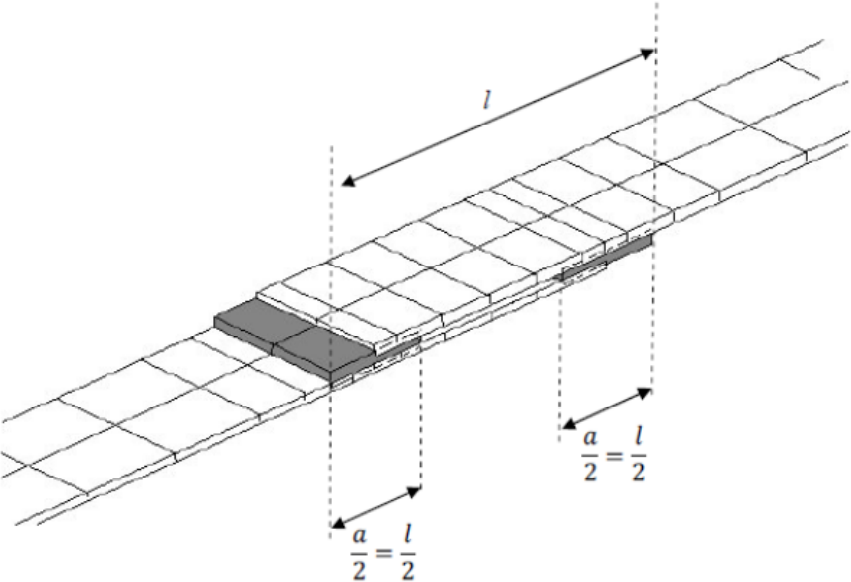


Figure 8

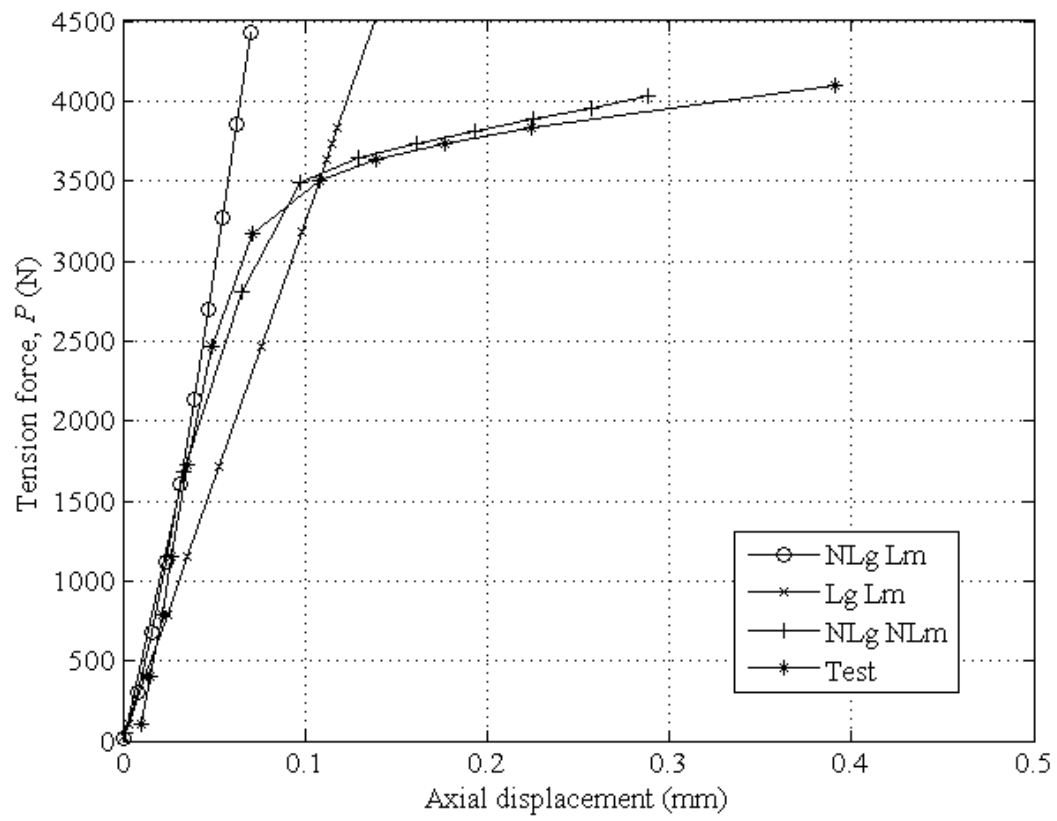


Figure 9

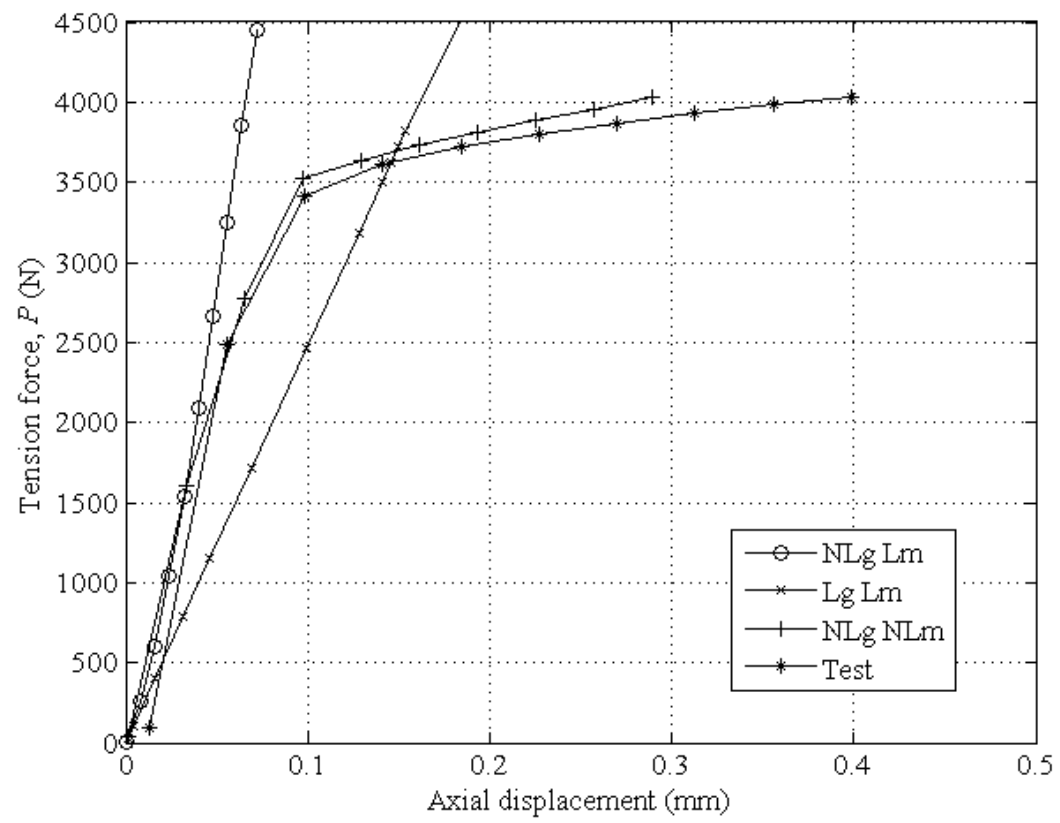


Figure 10

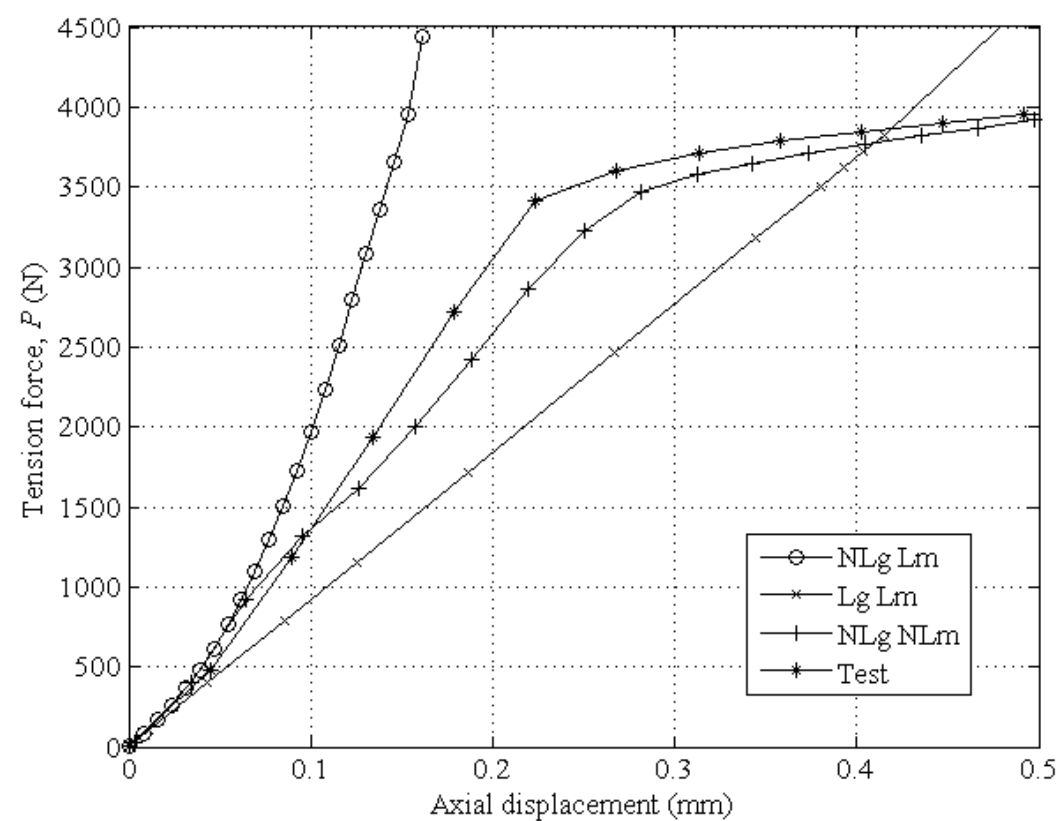


Figure 11

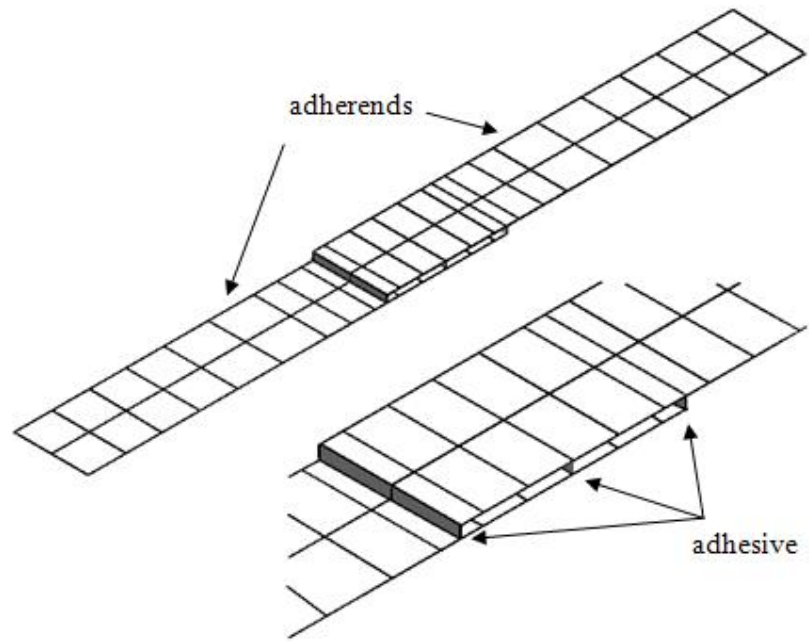


Figure 12

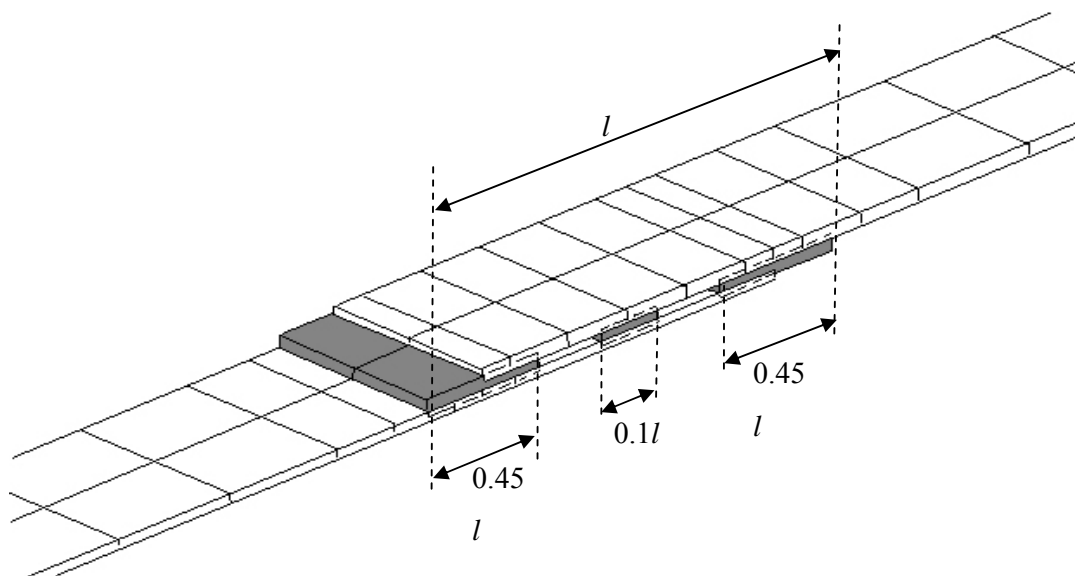


Figure 13